Conservation and restoration of St. George's church (Nördlingen, Germany), a 15th century Gothic church built using suevite from the Ries impact crater

Michael Heap, H. Albert Gilg, Kai-Uwe Hess, Lea Mertens, Gisela Pösges, Thierry Reuschlé

Conservation and restoration of St. George's church (Nördlingen, Germany), a 15th century Gothic church built using suevite from the Ries impact crater

Michael J. Heap*[1], H. Albert Gilg [2], K.-U. Hess[3], Lea Mertens[4], Gisela Pösges[5], and Thierry Reuschlé[1]

[1]*Géophysique Expérimentale, Institut de Physique de Globe de Strasbourg (UMR 7516 CNRS, Université de Strasbourg/EOST), 5 rue René Descartes, 67084 Strasbourg cedex, France.*

[2]*Lehrstuhl für Ingenieurgeologie, Technische Universität München, Munich, Germany.*

[3]*Earth and Environmental Sciences, Ludwig-Maximilians-Universität, Theresienstrasse 41, 80333 Munich, Germany.*

[4]*Wittner - Steinbearbeitung und Denkmalpflege, Nördlingen, Germany.*

[5]*Geopark Ries, Nördlingen, Germany.*

Corresponding author: Michael Heap (heap@unistra.fr)

Length of manuscript (excluding abstract, acknowledgements and references): 3052 words

Length of manuscript (including abstract, acknowledgements and references): 4961 words

Abstract

An asteroid impact in southwest Germany ca. 15 Ma left a >20 km-diameter blanket of poorly sorted clastic rock, called suevite. In the 15th century, the suevite was used to construct a Gothic church (St. George's church, Nördlingen). Visual inspection of the church highlights its strong weathering susceptibility. We investigate whether the suevite used to construct the church and the rocks used in its restoration (suevite and sandstone) are weaker when saturated with water, important for conservation strategies. We additionally assess, by comparing their physical properties, the suitability of the replacement stones. We show that the strength of the suevite used to build the church is reduced by half when water-saturated, considered here a consequence of its high smectite content. This helps explain the prevalent weathering of the stones forming the outer walls of the church. The replacement suevite has a higher wet/dry strength ratio than the original suevite and is therefore more resistant to weathering. Not only does the replacement sandstone have a low ratio of wet/dry strength, but also its physical properties are different from the original suevite, which has almost identical physical properties to those of the replacement suevite. Based on these results, and the appearance of the stones, we recommend that, where possible, natural suevite stones be used to replace the weathered blocks of suevite at St. George's church and at buildings built using suevite within the region.

Keywords: suevite; conservation; porosity; permeability; uniaxial compressive strength

1 Introduction

An asteroid impacted a 600-700 m thick layer of sedimentary rocks overlying a crystalline basement (Pohl et al., 1977; von Engelhardt, 1990; Stöffler et al., 2013) in southwest Germany ca. 15 Ma (Rocholl et al., 2018) (Fig. 1a). In the aftermath of the impact, "clouds" of hot debris and gas dispersed radially (Siegert et al., 2017) forming a subcircular blanket of poorly sorted clastic material that subsequently welded to form a rock called suevite. Two layers of suevite exist: (1) "crater suevite", which is up to 300 m thick and covered by Miocene lake sediments and (2) "outer suevite", which is only up to 25 m thick and outcrops up to 22 km from the centre of the structure (Stöffler et al., 2013). The Ries impact crater, a double-layer rampart crater (Sturm et al., 2013), has an inner- and outer-ring diameter of ca. 12 and 24 km, respectively (Wünnemann et al., 2005; Fig. 1b). The suevite contains centimetric-sized clasts of impact melt glass (aerodynamically shaped bombs and angular fragments; Stähle, 1972; Osinski, 2003) and crystalline and sedimentary rocks (Graup, 1981; von Engelhardt, 1990, 1997). These clasts are hosted within a matrix of clays (and sometimes zeolites) that formed as a result of post-deposition hydrothermal alteration, impact melt glass, rock and mineral fragments, and crystallites (Newsom et al., 1986; von Engelhardt, 1990, 1997; Osinski, 2005; Osinski et al., 2010; Muttik et al., 2010, 2011; Sapers et al., 2017). Coesite is also present (Stöffler, 1966; Stähle et al., 2008), the mineral that confirmed the impact origin of these deposits (Shoemaker and Chao, 1961). Diamond and other high-pressure minerals have also been identified (Stöffler et al., 2013).

The town of Nördlingen (Fig. 1) was founded within the impact crater and suevite was used in its construction. Parts of the city hall, the city fortifications (walls and gates), and the impressive 15th century Gothic church (St. George's church; Fig. 1c) were constructed using suevite. A visual inspection of St. George's church, and

other buildings constructed using suevite, highlights its strong weathering susceptibility. There is evidence of alveolisation (detachment of clasts/fragments), scaling, exfoliation, and disaggregation (Fig. 2a) and, as a result, many of the suevite dimension stones of St. George's church have been recently (starting from the 1970s) replaced with blocks of synthetic and natural suevite and a white sandstone (Fig. 2b and 2c).

Laboratory experiments on clay-bearing sandstones (Dyke and Dobereiner, 1991; Hawkins and McConnell, 1992; Shakoor and Barefield, 2009; Wasantha and Ranjith, 2014; Verstrynge et al., 2014; Heap et al., 2018a, 2019) and tuffs (e.g., Zhu et al., 2011; Heap et al., 2018b) suggest that clays may promote rock weakening in the presence of water. The metric "water-weakening", the ratio of the wet to dry strength of a material, is often used to describe this affect, where low values (close to zero) indicate a strong water-weakening effect and values at or close to unity indicate that there is little or no water-weakening. The high clay content of the suevite (Newsom et al., 1986; Osinski, 2005; Muttik et al., 2010, 2011; Sapers et al., 2017) may therefore help explain its high susceptibility to weathering (Fig. 2).

2 Research aim

Our objective is twofold. First, to inform on the suitability of the replacement stones (Přikryl, 2007), we assess the physical properties of the suevite originally used in the construction of the church and the replacement suevite and sandstone. Second, to better understand the observed weathering susceptibility (Fig. 2), we assess the water-weakening of the original suevite and the replacement stones.

3 Materials and methods

The two suevite blocks used in this study were sourced from the quarries at Altenbürg (thought to be the quarry from where the rock for the church was sourced; Fig. 1b) and Seelbronn (the quarry from where the suevite used to restore the church is sourced; Fig. 1b; see also Poschlod et al., 2017). Although the Altenbürg quarry is thought to be the source site for the suevites used in the original construction, it cannot be definitively ruled out that some blocks were sourced from other quarries. Nevertheless, we consider that the block we collected from Altenbürg well represents the colour and therefore alteration of the blocks used in the original construction. The sandstone used in the restoration of the church is Schönbrunn sandstone (from Schönbrunn-Hermannsberg quarry in Bavaria, Germany).

Both suevites are poorly sorted clastic rocks that contain millimetric and centimetric-sized clasts of glass (aerodynamically shaped bombs and angular fragments), crystalline rocks (Variscan granites and pre-Variscan gneisses and amphibolites), and sedimentary rocks within a fine-grained matrix (von Engelhardt, 1990, 1997; Stöffler et al., 2013). Macroscopically, the only observable difference between the blocks is that the suevite blocks from Seelbronn and Altenbürg are blue-grey and yellow-green in colour, respectively (Figs. 2 and 3). The replacement sandstone is very well sorted and contains faint bedding-parallel laminations.

A total of 62 cylindrical samples were cored from the three blocks: 20 samples of Schönbrunn sandstone (SBS), 20 samples of suevite from Seelbronn (SEEL), and 22 samples of suevite from Altenbürg (ALT). The sandstone samples were cored to a diameter of 20 mm and cut and precision-ground to a nominal length of 40 mm. Due to the heterogeneity of the suevite blocks, the suevite samples were prepared to a diameter of 25 mm and cut and precision-ground to a nominal length of 60 mm. The suevite samples were cored so as to avoid centimetric-sized clasts. Although these sample

dimensions do not conform to standard guidelines, such as those outlined by the International Society for Rock Mechanics and Rock Engineering (ISRM; Ulusay, 2014), we highlight that (1) the grain size of our materials is significantly smaller than our sample diameters and (2) a recent study has shown that the uniaxial compressive strength (UCS) of small (diameter = 8-9 mm) samples was very similar to that determined from standard-sized samples (Van Stappen et al., 2019).

The connected porosity of each sample was then determined using the skeletal (connected) volume of the sample given by a helium pycnometer and the bulk volume calculated using the sample dimensions. The permeability of select samples was measured using a benchtop nitrogen-gas permeameter (see Farquharson et al., 2016; Heap and Kennedy, 2016). Permeability measurements were performed at room temperature under a confining pressure of 1 MPa (for more information on such measurements, see Heap et al., 2017).

Finally, the samples were deformed in a uniaxial loadframe at a strain rate of 1.0×10^{-5} s^{-1} until macroscopic failure. The UCS of a material is a commonly used strength metric in engineering geoscience. Half of each sample suite was deformed "wet" (vacuum-saturated in deionised water and deformed in a water bath) and the other half deformed "dry" (dried in a vacuum-oven for at least 48 hours prior to deformation). The water saturation procedure for the samples deformed wet consisted of two steps. First, the vacuum-dried samples were placed inside a belljar that was then evacuated for at least 12 hours. Second, degassed deionised water was introduced into the bell jar whilst under vacuum. This procedure ensured that the void space within the rock was completely water-saturated.

The mineral content of the studied materials was quantified using X-ray powder diffraction (XRPD). Crushed sample pieces were ground in isopropanol with a

McCrone micronizing mill using agate cylinders, and 10 wt.% ZnO was added (internal standard). The analyses were performed on side-loaded powder mounts using a PW 1800 X-ray diffractometer (Cu-Ka, 40 kV, 30 mA, automatic divergence slit, irradiated length 10 mm, 2-70° 2q, step width 0.02°, counting time 1 s per step, graphite monochromator). The mineral phases were quantified using the Rietveld program BGMN (Bergmann et al., 1998). To identify the clay minerals, we also separated < 2 μm fractions by gravitational settling and prepared oriented mounts that were X-rayed in an air-dried and ethylene-glycolated state. The carbonate contents of the suevite samples were additionally quantified using a Hecatech EURO elemental analyser.

To complement our XRPD analyses, thermo-gravimetric (TG) analyses were performed using a Netzsch STA 449 C thermobalance apparatus. Powdered samples were heated in an argon atmosphere at a rate of 10 °C/min up to a temperature of 1000 °C and then cooled back to room temperature at the same rate.

A thin section (~30 μm-thick) of each the suevite blocks was prepared and their microstructure was examined using a TESCAN VEGA II XMU scanning electron microscope (SEM) (using a beam voltage of 150 kW and a working distance of 23 mm). Minerals were identified during our SEM analyses using energy-dispersive X-ray spectroscopy.

4 Results

4.1 Mineral content and microstructure

Schönbrunn sandstone is a feldspathic sandstone that contains small quantities of muscovite and chlorite (Table 1). The suevites from Seelbronn and Altenbürg are both principally composed of amorphous phases, smectite, and plagioclase, with minor quantities of quartz, coesite, K-feldspar, calcite, biotite, and hematite (Table 1). The

only noteworthy differences are that Seelbronn suevite contains more plagioclase than Altenbürg suevite (27 and 18 wt.%, respectively; Table 1) and that Altenbürg suevite contains more calcite (13 ± 1 and 2.1 ± 0.2 wt.%, respectively; Table 1). The calcite content of both suevite samples was determined by the elemental analyser to be 14.0 ± 0.1 and 2.11 ± 0.06 wt.%, respectively, confirming the results of the XRPD analyses. The mineralogical composition of our suevites is in agreement with previous studies (Engelhardt, 1997; Osinski, 2005; Sapers et al., 2017).

The results of the TG analysis (Fig. 4a) corroborate our XRPD data. The mass loss seen at ~700-750 °C in both suevites, associated with the decomposition of calcite (Samtani et al., 2002), is much more pronounced for the Altenbürg suevite than for the Seelbronn suevite. The mass loss < 700 °C in both suevites is associated with the dehydration (~100-150 °C) and dehydroxylation (~400-600 °C) of smectite (Girgis et al., 1987), abundant in these materials (Table 1). The mass loss in Schönbrunn sandstone between ~500-550 °C is associated with the dehydroxylation of chlorite (Ross and Kodama, 1976).

Backscattered SEM images of the thin sections prepared from the two suevite blocks are provided in Fig. 3. The suevite blocks are microstructurally complex, containing poorly sorted angular fragments (of quartz, calcite, K-feldspar, plagioclase) within a fine-grained matrix. The images also show that both suevites are pervasively microcracked.

4.2 Petrophysical data

The average connected porosities of Altenbürg suevite, Seelbronn suevite, and Schönbrunn sandstone are 0.238, 0.245, and 0.163, respectively (Table 2). The average

permeability of both suevites is ~2 × 10^{-15} m^2, and the permeability of a sample of Schönbrunn sandstone was measured to be 4.69 × 10^{-16} m^2 (Table 2).

Our mechanical data show that the suevite from the Seelbronn quarry is stronger than that from Altenbürg, and that the sandstone is much stronger (about twice as strong) than both suevites (Fig. 4b; Table 2). The average dry and wet strengths of the suevites from Seelbronn and Altenbürg are 34.2 (standard deviation, s. d., 11.2 MPa) and 29.2 (s. d. 5.8 MPa) MPa and 24.2 (s. d. 6.2 MPa) and 16.3 (s. d. 4.1 MPa) MPa, respectively (Fig. 4b). We consider the difference in strength between samples cored from the same block (standard deviations shown in Fig. 4b) to be a result of natural sample-to-sample variability. The average dry and wet strength of the sandstone is 59.3 (s. d. 2.4 MPa) and 30.6 (s. d. 0.5 MPa) MPa, respectively. The ratio of wet to dry strength is 0.71, 0.56, and 0.52, respectively, for Seelbronn suevite, Altenbürg suevite, and Schönbrunn sandstone.

5 Discussion

5.1 Weathering of the suevite at St. George's church

The study of Heap et al. (2019) compiles the available data for water-weakening in sandstone and shows that the ratio of wet to dry strength in sandstone decreases as clay content is increased. The water-weakening of sandstone was considered by these authors to be the result of a reduction in fracture surface free energy in the presence of water and that, due to the ability of clays to adsorb water, higher clay contents ensured that more water was adsorbed on the surface of growing microcracks. We similarly conclude here that the presence of clays within the rock matrix (~25 wt.%; Table 1) is largely responsible for the observed water-weakening in the studied suevites. We additionally conclude that the lower ratio of wet to dry strength in the Altenbürg

220 suevite, compared to the Seelbronn suevite, is a result of the slightly higher wt.% of
221 smectite (Table 1) and the higher wt.% of calcite (Table 1), another mineral considered
222 to weaken in the presence of water (Baud et al., 2009, 2016) (although we anticipate
223 that clay contributes more to the observed water-weakening than calcite). Due to the
224 absence of clay, the very low ratio of wet to dry strength of 0.52 for Schönbrunn
225 sandstone is unexpected (Fig. 4c). Possible reasons for the observed water-weakening
226 include: (1) the presence of minor (4 wt.%; Table 1) chlorite (a hydrated phyllosilicate
227 mineral), (2) a reduction in the fracture toughness of feldspar, which is relatively
228 abundant (35 wt.%; Table 1), and (3) a decrease in capillary pressure or an increase in
229 pore pressure (e.g., Verstrynge et al., 2014); however, we highlight that a permeability
230 of ~5×10^{-16} m^2 (Table 2) is likely high enough to ensure drained deformation. More
231 data are required to forward a definitive reason for the high water-weakening observed
232 in Schönbrunn sandstone.

233 The suevite from Seelbronn has a higher ratio of wet to dry strength than
234 Altenbürg suevite (0.71 and 0.56, respectively; Fig. 4b; Table 2) and could help explain
235 the observed weathering susceptibility (Fig. 2). Some of the outer walls however, such
236 as the wall on the east side, are noticeably less weathered and likely reflect variations
237 in stone alteration and environmental factors. Variation in the alteration of the stones
238 used is not only visible by the different colours of the blocks (Fig. 2), but also expected
239 due the preferential selection of medium-sized (typically 2-3 m in size) blocks
240 ("bollen"), regardless of their degree of alteration, by medieval stonemasons. In the
241 absence of modern cutting tools, these 2-3 m-sized blocks were easier to manage for
242 medieval stonemasons. It is possible therefore that the blocks forming the east side of
243 the church were sourced from a part of the quarry that was less altered (or even that
244 they were sourced, or partly sourced, from another quarry). Nowadays, cuboids are cut

from larger bollen (as large as 5-10 m), allowing stonemasons to assess the extent of alteration and therefore stone quality. Environmental factors could have also influenced the variation in weathering seen on different church faces. Swelling clays (Table 1) and micropores (Fig. 3), for example, can lead to building stone deterioration during wetting/drying cycles (Wangler and Scherer, 2008; Wrangler et al., 2011; Ruedrich et al., 2011; Colas et al., 2011). In the case of St. George's church, it is the south-facing side that will, on average, receive the most sunlight and is therefore most prone to solar-induced rock weathering (Eppes et al., 2016). Since the prevailing wind direction is from west, as deduced from yearly weather reports for Nördlingen, it is the west-facing side that should receive more wind-driven rainfall. Freeze-thaw damage (average minimum temperatures are below 0 °C in the winter months) should also affect the sides of the church that receive the most precipitation and the least sunlight. We note that the tensile strength of materials, often invoked as the principal metric in, for example, freeze-thaw weathering (Nicholson and Nicholson, 2000), is typically a tenth or a twelfth of the UCS (Paterson and Wong, 2005), the strength metric reported herein.

5.2 The use of replacement stones at St. George's church

Some of the original suevite blocks forming St. George's church (Fig. 1c) have been recently replaced with synthetic and natural suevite and sandstone (Fig. 2). It is recommended that damaged or weathered stones be replaced by new stones sourced from the same quarry or, if this is not possible, using stone with similar petrophysical properties is strongly advised (Přikryl, 2007). It is further recommended, from an aesthetic and cultural point of view, that the replacement stones have a similar appearance (colour and texture) to the original stones (Přikryl, 2007). To this end, there are many studies that have investigated the physical properties (e.g., porosity, saturation

and capillary absorption coefficients, elastic wave velocity, compressive and flexural strengths) of replacement stones for monuments and buildings of historical significance (Nijland et al., 2010; Graue et al., 2011; Quist et al., 2013; De Kock et al., 2013, 2015). Our petrophysical assessment shows that the Schönbrunn sandstone is less porous, about an order of magnitude less permeable, and more than twice as strong (in dry conditions; Fig. 4b) than the original suevite used in the construction of the church (Table 2). We also note that the Schönbrunn sandstone is very different in appearance to the original suevite (Fig. 2). By contrast, the physical properties and appearance of the original suevite and the natural suevite used in the restoration of the church are very similar (Table 2). Based on our petrophysical analyses, and a visual assessment of the appearance of the stones, we recommend, where possible, that the original damaged or weathered suevite stones be replaced with natural suevite from the currently active Seelbronn quarry.

6 Conclusions

We provide herein experimental data to better understand (1) the observed weathering susceptibility of suevite and (2) the suitability of the replacement stones used in the restoration of St. George's church in Nördlingen. We find that the strength of the suevite originally used to build the church is reduced by about half when water-saturated, considered here as a result of its high smectite content. This helps explain the prevalent weathering of the stones forming the outer walls of the church. Due to its low ratio of wet to dry strength, large differences between its physical properties and those of the original suevite dimension stone, and visual differences, Schönbrunn sandstone is not considered here as an ideal replacement stone. By contrast, the suevite replacement stone from the quarry at Seelbronn is more resistant to weathering when

295 water-saturated and has a similar appearance and similar physical properties to the
296 original suevite. We therefore recommend that, where possible, natural suevite stones
297 be used to replace the weathered blocks of original suevite at St. George's church and
298 at buildings built using suevite within the area.
299
300 **Acknowledgements**
301 The first author acknowledges a Prix d'Espoirs grant, awarded by the University
302 of Strasbourg. We warmly thank Olivier Lengliné, who chauffeured the first author to
303 and from Nördlingen. We thank Bertrand Renaudié, Alexandra Kushnir, Matthias
304 Wittner, Werner Häusler, and Adrian Jones. The constructive comments of the
305 associate editor and two anonymous reviewers helped improve this manuscript.
306

References

Baud, P., Vinciguerra, S., David, C., Cavallo, A., Walker, E., & Reuschlé, T. (2009). Compaction and failure in high porosity carbonates: Mechanical data and microstructural observations. In *Rock Physics and Natural Hazards* (pp. 869-898). Birkhäuser Basel.

Baud, P., Rolland, A., Heap, M., Xu, T., Nicolé, M., Ferrand, T., Reuschlé, T., Toussaint, R. and Conil, N. (2016). Impact of stylolites on the mechanical strength of limestone. *Tectonophysics*, *690*, 4-20.

Bergmann, J., Friedel, P., & Kleeberg, R. (1998). BGMN—a new fundamental parameters based Rietveld program for laboratory X-ray sources, its use in quantitative analysis and structure investigations. *CPD Newsletter*, *20*(5).

Colas, E., Mertz, J. D., Thomachot-Schneider, C., Barbin, V., & Rassineux, F. (2011). Influence of the clay coating properties on the dilation behavior of sandstones. Applied Clay Science, 52(3), 245-252.

De Kock, T., Dewanckele, J., Boone, M., De Schutter, G., Jacobs, P., & Cnudde, V. (2013). Replacement stones for Lede stone in Belgian historical monuments. *Geological Society, London, Special Publications*, *391*, SP391-9.

De Kock, T., De Boever, W., Dewanckele, J., Boone, M. A., Jacobs, P., & Cnudde, V. (2015). Characterization, performance and replacement stone compatibility of building stone in the 12th century tower of Dudzele (Belgium). *Engineering Geology*, *184*, 43-51.

Dyke CG, Dobereiner L (1991) Evaluating the strength and deformability of sandstones. Quarterly Journal of Engineering Geology and Hydrogeology 24:123-134.

Eppes, M. C., Magi, B., Hallet, B., Delmelle, E., Mackenzie-Helnwein, P., Warren, K., & Swami, S. (2016). Deciphering the role of solar-induced thermal stresses in rock weathering. Bulletin, 128(9-10), 1315-1338.

Farquharson, J. I., Heap, M. J., Lavallée, Y., Varley, N. R., & Baud, P. (2016). Evidence for the development of permeability anisotropy in lava domes and volcanic conduits. *Journal of Volcanology and Geothermal Research*, *323*, 163-185.

Girgis, B. S., El-Barawy, K. A., & Felix, N. S. (1987). Dehydration kinetics of some smectites: a thermogravimetric study. *Thermochimica Acta*, *111*, 9-19.

Graup, G. (1981). Terrestrial chondrules, glass spherules and accretionary lapilli from the suevite, Ries Crater, Germany. *Earth and Planetary Science Letters*, *55*, 407-418.

Graue, B., Siegesmund, S., & Middendorf, B. (2011). Quality assessment of replacement stones for the Cologne Cathedral: mineralogical and petrophysical requirements. *Environmental Earth Sciences*, *63*(7-8), 1799-1822.

Hawkins AB, McConnell BJ (1992) Sensitivity of sandstone strength and deformability to changes in moisture content. Quarterly Journal of Engineering Geology and Hydrogeology 25:115-30.

Heap, M. J., & Kennedy, B. M. (2016). Exploring the scale-dependent permeability of fractured andesite. *Earth and Planetary Science Letters*, *447*, 139-150.

Heap, M. J., Kushnir, A. R., Gilg, H. A., Wadsworth, F. B., Reuschlé, T., & Baud, P. (2017). Microstructural and petrophysical properties of the Permo-Triassic sandstones (Buntsandstein) from the Soultz-sous-Forêts geothermal site (France). *Geothermal Energy*, *5*(1), 26.

Heap, M. J., Reuschlé, T., Kushnir, A. R., & Baud, P. (2018a). The influence of hydrothermal brine on the short-term strength and elastic modulus of sandstones from exploration well EPS-1 at Soultz-sous-Forêts (France). Geothermal Energy, 6(1), 29.

353 Heap, M. J., Farquharson, J. I., Kushnir, A. R., Lavallée, Y., Baud, P., Gilg, H. A., & Reuschlé,
354 T. (2018b). The influence of water on the strength of Neapolitan Yellow Tuff, the most
355 widely used building stone in Naples (Italy). *Bulletin of Volcanology*, *80*:51.
356 Heap MJ, Villeneuve M, Kushnir ARL, Farquharson JI, Baud P, Reuschlé T (2019) Rock mass
357 strength and elastic modulus of the Buntsandstein: an important lithostratigraphic unit
358 for geothermal exploitation in the Upper Rhine Graben. *Geothermics*, 77, 236-256.
359 Muttik, N., Kirsimäe, K., & Vennemann, T. W. (2010). Stable isotope composition of smectite
360 in suevites at the Ries crater, Germany: Implications for hydrous alteration of
361 impactites. *Earth and Planetary Science Letters*, *299*(1-2), 190-195.
362 Muttik, N., Kirsimäe, K., Newsom, H. E., & Williams, L. B. (2011). Boron isotope composition
363 of secondary smectite in suevites at the Ries crater, Germany: boron fractionation in
364 weathering and hydrothermal processes. *Earth and Planetary Science Letters*, *310*(3-4),
365 244-251.
366 Newsom, H. E., Graup, G., Sewards, T., & Keil, K. (1986). Fluidization and hydrothermal
367 alteration of the suevite deposit at the Ries crater, West Germany, and implications for
368 Mars. *Journal of Geophysical Research: Solid Earth*, *91*(B13), E239-E251.
369 Nicholson, D. T., & Nicholson, F. H. (2000). Physical deterioration of sedimentary rocks
370 subjected to experimental freeze–thaw weathering. Earth Surface Processes and
371 Landforms: The Journal of the British Geomorphological Research Group, 25(12), 1295-
372 1307.
373 Nijland, T. G., Van Hees, R. P., & Bolondi, L. (2010). Evaluation of three Italian tuffs
374 (Neapolitan Yellow Tuff, Tufo Romano and Tufo Etrusco) as compatible replacement
375 stone for Römer tuff in Dutch built cultural heritage. *Geological Society, London,*
376 *Special Publications*, *333*(1), 119-127.
377 Osinski, G. R. (2003). Impact glasses in fallout suevites from the Ries impact structure,
378 Germany: An analytical SEM study. *Meteoritics & Planetary Science*, *38*(11), 1641-
379 1667.
380 Osinski, G. R., Grieve, R. A., & Spray, J. G. (2004). The nature of the groundmass of surficial
381 suevite from the Ries impact structure, Germany, and constraints on its
382 origin. *Meteoritics & Planetary Science*, *39*(10), 1655-1683.
383 Osinski, G. R. (2005). Hydrothermal activity associated with the Ries impact event,
384 Germany. *Geofluids*, *5*(3), 202-220.
385 Paterson, M. S., & Wong, T. F. (2005). Experimental rock deformation-the brittle field.
386 Springer Science & Business Media.
387 Pohl, J., Stoeffler, D., Gall, H. V., & Ernstson, K. (1977). The Ries impact crater. In *Impact*
388 *and explosion cratering: Planetary and terrestrial implications* (pp. 343-404).
389 Poschlod, K., Pfeiffer, R., Bittner, S., Krug, R., Lehrberger, G., and Sutterer, V. (2017).
390 Erfassung historischer Naturwerksteinvorkommen als Grundlage für deren
391 umweltverträgliche Reaktivierung zwecks Restaurierung national bedeutender
392 Kulturgüter in Bayern. https://doi.org/10.24359/dbu.31549.
393 Přikryl, R. (2007). Understanding the earth scientist's role in the pre-restoration research of
394 monuments: an overview. *Geological Society, London, Special Publications*, *271*(1), 9-
395 21.
396 Quist, W. J., Nijland, T. G., & Van Hees, R. P. J. (2013). Replacement of Eocene white sandy
397 limestone in historical buildings: over 100 years of practice in the Netherlands.
398 Geological Society of London.
399 Rocholl, A., Böhme, M., Gilg, H. A., Pohl, J., Schaltegger, U., & Wijbrans, J. (2018). Comment
400 on “A high-precision 40 Ar/39 Ar age for the Nördlinger Ries impact crater, Germany,

and implications for the accurate dating of terrestrial impact events" by Schmieder et al. (Geochimica et Cosmochimica Acta 220 (2018) 146-157. *Geochimica et Cosmochimica Acta*.

Ross, G. J., & Kodama, H. (1976). Experimental alteration of a chlorite into a regularly interstratified chlorite-vermiculite by chemical oxidation. *Clays and Clay Minerals*, *24*(4), 183-190.

Ruedrich, J., Bartelsen, T., Dohrmann, R., & Siegesmund, S. (2011). Moisture expansion as a deterioration factor for sandstone used in buildings. Environmental Earth Sciences, 63(7-8), 1545-1564.

Samtani, M., Dollimore, D., & Alexander, K. S. (2002). Comparison of dolomite decomposition kinetics with related carbonates and the effect of procedural variables on its kinetic parameters. *Thermochimica Acta*, *392*, 135-145.

Sapers, H. M., Osinski, G. R., Flemming, R. L., Buitenhuis, E., Banerjee, N. R., Tornabene, L. L., Blain, S., Hainge, J. (2017). Evidence for a spatially extensive hydrothermal system at the Ries impact structure, Germany. *Meteoritics & Planetary Science*, 52(2), 351-371.

Shakoor, A., & Barefield, E. H. (2009). Relationship between unconfined compressive strength and degree of saturation for selected sandstones. *Environmental & Engineering Geoscience*, *15*(1), 29-40.

Shoemaker, E. M., & Chao, E. C. (1961). New evidence for the impact origin of the Ries Basin, Bavaria, Germany. *Journal of Geophysical Research*, *66*(10), 3371-3378.

Siegert, S., Branney, M. J., & Hecht, L. (2017). Density current origin of a melt-bearing impact ejecta blanket (Ries suevite, Germany). *Geology*, *45*(9), 855-858.

Stähle, V. (1972). Impact glasses from the suevite of the Nördlinger Ries. *Earth and Planetary Science Letters*, *17*(1), 275-293.

Stähle, V., Altherr, R., Koch, M., & Nasdala, L. (2008). Shock-induced growth and metastability of stishovite and coesite in lithic clasts from suevite of the Ries impact crater (Germany). *Contributions to Mineralogy and Petrology*, *155*(4), 457-472.

Stöffler, D. (1966). Zones of impact metamorphism in the crystalline rocks of the Nördlinger Ries crater. *Contributions to Mineralogy and Petrology*, *12*(1), 15-24.

Stöffler, D., Artemieva, N. A., Wünnemann, K., Reimold, W. U., Jacob, J., Hansen, B. K., Summerson, I. A. (2013). Ries crater and suevite revisited—Observations and modeling Part I: Observations. *Meteoritics & Planetary Science*, 48(4), 515-589.

Sturm, S., Wulf, G., Jung, D., & Kenkmann, T. (2013). The Ries impact, a double-layer rampart crater on Earth. *Geology*, *41*(5), 531-534.

Ulusay, R. (Ed.). (2014). The ISRM suggested methods for rock characterization, testing and monitoring: 2007-2014. Springer.

Van Stappen, J. F., De Kock, T., De Schutter, G., & Cnudde, V. (2019). Uniaxial compressive strength measurements of limestone plugs and cores: a size comparison and X-ray CT study. Bulletin of Engineering Geology and the Environment, 1-10.

Verstrynge, E., Adriaens, R., Elsen, J., & Van Balen, K. (2014). Multi-scale analysis on the influence of moisture on the mechanical behavior of ferruginous sandstone. Construction and Building Materials, 54, 78-90.

Von Engelhardt, W. (1990). Distribution, petrography and shock metamorphism of the ejecta of the Ries crater in Germany—A review. *Tectonophysics*, *171*(1-4), 259-273.

Von Engelhardt, W. (1997). Suevite breccia of the Ries impact crater, Germany: Petrography, chemistry and shock metamorphism of crystalline rock clasts. *Meteoritics & Planetary Science*, *32*(4), 545-554.

448 Wasantha PL, Ranjith PG (2014) Water-weakening behavior of Hawkesbury sandstone in
449 brittle regime. Engineering Geology 178:91-101.
450 Wangler, T., & Scherer, G. W. (2008). Clay swelling mechanism in clay-bearing sandstones.
451 Environmental Geology, 56(3-4), 529-534.
452 Wangler, T. P., Stratulat, A., Duffus, P., Prévost, J. H., & Scherer, G. W. (2011). Flaw
453 propagation and buckling in clay-bearing sandstones. Environmental Earth Sciences,
454 63(7), 1565-1572.
455 Wünnemann, K., Morgan, J. V., & Jödicke, H. (2005). Is Ries crater typical for its size? An
456 analysis based upon old and new geophysical data and numerical modeling. In *Large*
457 *meteorite impacts III* (Vol. 384, pp. 67-84). Geological Society of America.
458 Zhu, W., Baud, P., Vinciguerra, S., & Wong, T. F. (2011). Micromechanics of brittle faulting
459 and cataclastic flow in Alban Hills tuff. *Journal of Geophysical Research: Solid*
460 *Earth*, *116*(B6).

461 **Table 1.** Quantitative bulk mineralogical composition, determined using X-ray powder
462 diffraction (XRPD), for the three materials used in this study. The error associated with
463 the estimation of the content of amorphous phases is a conservative estimate (it has not
464 been calculated).

465

Mineral	Altenbürg suevite (values in wt.%)	Seelbronn suevite (values in wt.%)	Schönbrunn sandstone (values in wt.%)
Quartz	9 ± 1	10 ± 1	57 ± 2
Coesite	1.7 ± 0.3	1.4 ± 0.3	-
K-feldspar	3.1 ± 0.5	1.7 ± 0.5	18 ± 2
Plagioclase	18 ± 2	27 ± 3	17 ± 2
Calcite	13 ± 1	2.1 ± 0.2	-
Smectite	25 ± 3	23 ± 3	-
Muscovite	-	-	4 ± 1
Chlorite	-	-	4 ± 1
Biotite	2.0 ± 0.5	1.9 ± 0.5	-
Hematite	0.2 ± 0.1	0.2 ± 0.1	-
Amorphous phases	28 ± 5	33 ± 5	-

466

467 **Table 2.** Experimental summary. SBS—Schönbrunn sandstone. ALT—Altenbürg
468 suevite. SEEL—Seelbronn suevite. Wet—vacuum-saturated in deionised water (see
469 text for details). Dry—dried in a vacuum oven at 40 °C for at least 48 h.
470

Sample	Connected porosity	Uniaxial compressive strength [MPa]	Experimental condition	Permeability [m^2]
SBS-1	0.16	31.7	Wet	-
SBS-2	0.16	62.6	Dry	-
SBS-3	0.16	30.0	Wet	-
SBS-4	0.16	30.8	Wet	-
SBS-5	0.16	60.2	Dry	4.69×10^{-16}
SBS-6	0.16	30.5	Wet	-
SBS-7	0.16	59.1	Dry	-
SBS-8	0.16	31.2	Wet	-
SBS-9	0.16	29.9	Wet	-
SSB-10	0.16	30.8	Wet	-
SBS-11	0.16	30.6	Wet	-
SBS-12	0.16	55.0	Dry	-
SBS-13	0.16	62.0	Dry	-
SBS-14	0.16	30.3	Wet	-
SBS-15	0.16	60.8	Dry	-
SBS-16	0.16	59.8	Dry	-
SBS-17	0.17	58.4	Dry	-
SBS-18	0.16	58.5	Dry	-
SBS-19	0.17	30.5	Wet	-
SBS-20	0.17	56.2	Dry	-
ALT-1	0.24	31.7	Dry	1.02×10^{-15}
ALT-2	0.26	31.6	Dry	2.54×10^{-15}
ALT-3	0.26	13.4	Wet	2.44×10^{-15}
ALT-4	0.23	25.3	Dry	3.13×10^{-15}
ALT-5	0.24	18.3	Wet	1.76×10^{-15}
ALT-6	0.26	17.7	Dry	3.16×10^{-15}
ALT-7	0.24	21.0	Wet	1.19×10^{-15}
ALT-8	0.26	22.5	Dry	1.84×10^{-15}
ALT-9	0.26	18.1	Wet	2.13×10^{-15}
ALT-10	0.23	33.0	Dry	9.54×10^{-16}
ALT-11	0.18	-	-	-
ALT-12	0.24	34.8	Dry	-
ALT-13	0.22	33.6	Dry	-
ALT-14	0.24	34.6	Dry	-
ALT-15	0.25	26.9	Dry	-
ALT-16	0.14	-	-	-
ALT-17	0.25	14.3	Wet	-
ALT-18	0.24	18.6	Wet	-
ALT-19	0.23	9.9	Wet	-

ALT-20	0.22	16.2	Wet	-
ALT-21	0.26	10.9	Wet	-
ALT-22	0.25	22.2	Wet	-
SEEL-1	0.27	18.4	Dry	6.33×10^{-15}
SEEL-2	0.23	48.6	Dry	6.22×10^{-16}
SEEL-3	0.27	-	-	5.68×10^{-15}
SEEL-4	0.25	21.7	Dry	7.40×10^{-16}
SEEL-5	0.22	42.2	Dry	9.53×10^{-16}
SEEL-6	0.21	31.1	Wet	1.08×10^{-15}
SEEL-7	0.23	30.9	Wet	1.47×10^{-15}
SEEL-8	0.23	32.8	Dry	6.32×10^{-16}
SEEL-9	0.27	17.4	Wet	1.47×10^{-15}
SEEL-10	0.23	43.3	Dry	5.84×10^{-16}
SEEL-11	0.26	-	-	-
SEEL-12	0.23	32.8	Dry	-
SEEL-13	0.22	31.0	Wet	-
SEEL-14	0.25	16.3	Wet	-
SEEL-15	0.25	22.7	Wet	-
SEEL-16	0.25	-	-	-
SEEL-17	0.26	20.4	Wet	-
SEEL-18	0.21	25.1	Wet	-
SEEL-19	0.23	24.3	Wet	-
SEEL-20	0.23	34.1	Dry	-

471

472 **Figures**

473

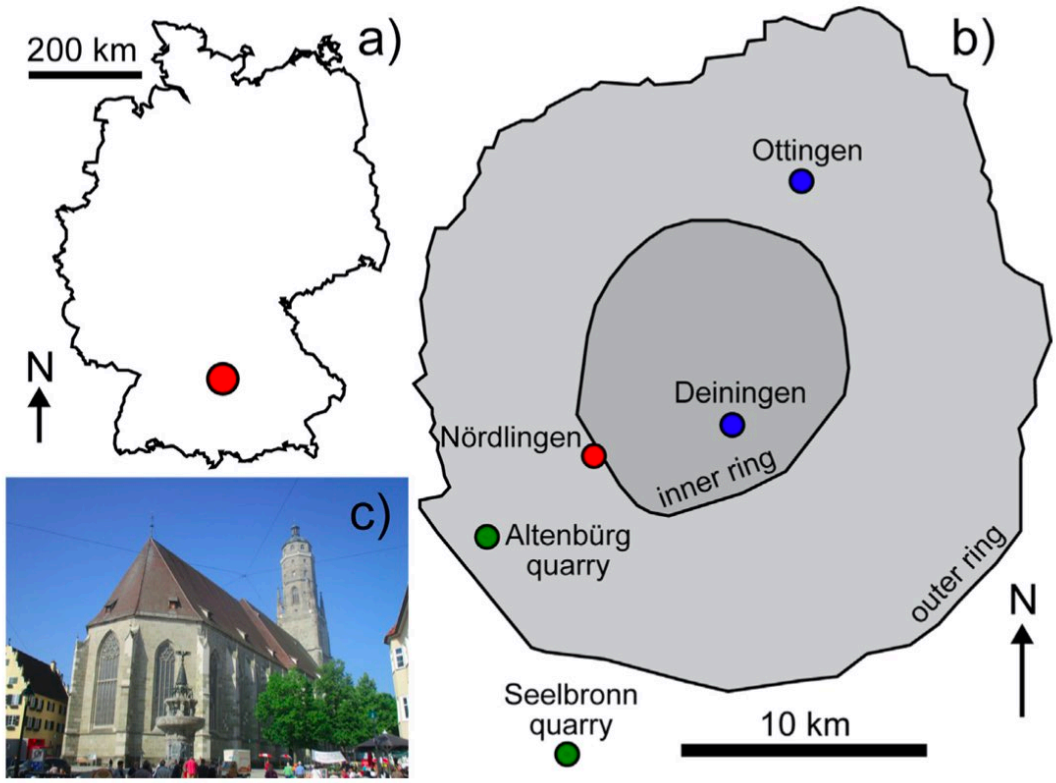

474

475 **Fig. 1**. (a) Map of Germany showing the location of Nördlingen (red circle). (b) Outline
476 of the Ries impact crater showing the position of Nördlingen (red circle), neighbouring
477 towns (blue circles), and the suevite quarries (green circles). (c) Photograph of St.
478 George's church (Nördlingen, Germany).

Fig. 2. (a) Photograph of the exterior wall of St. George's church (Nördlingen, Germany) showing an example of the original weathered suevite. Olivier Lengliné for scale. (b) Photograph of the exterior wall of St. George's church showing the replacement synthetic suevite and Schönbrunn sandstone. (c) Photograph of the exterior wall of St. George's church showing the replacement suevite from the quarry at Seelbronn.

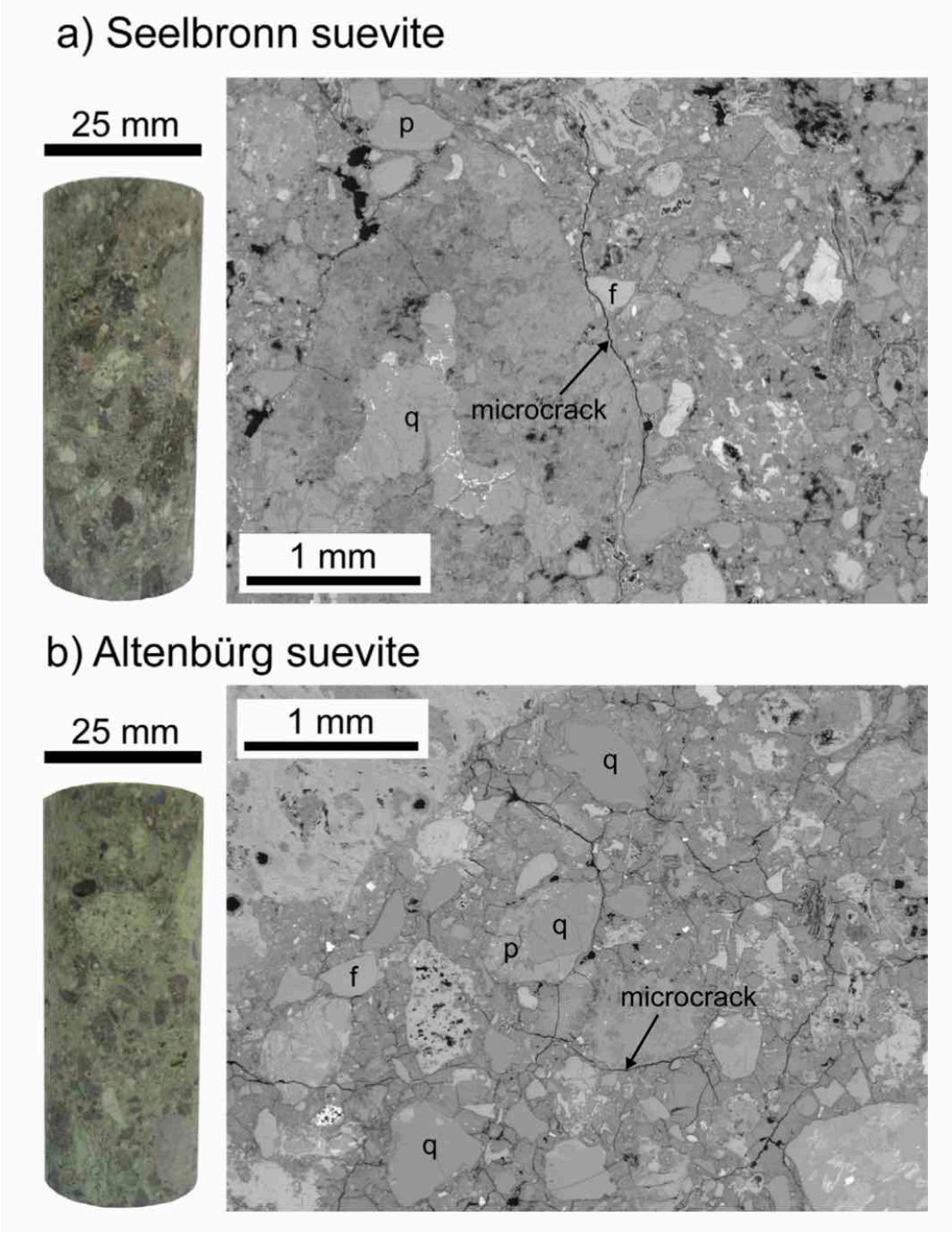

Fig. 3. (a) Photograph of cylindrical sample of Seelbronn suevite alongside a backscattered scanning electron microscope image of Seelbronn suevite. (b) Photograph of cylindrical sample of Altenbürg suevite alongside a backscattered scanning electron microscope image of Altenbürg suevite. f—K-feldspar. p—plagioclase. q—quartz.

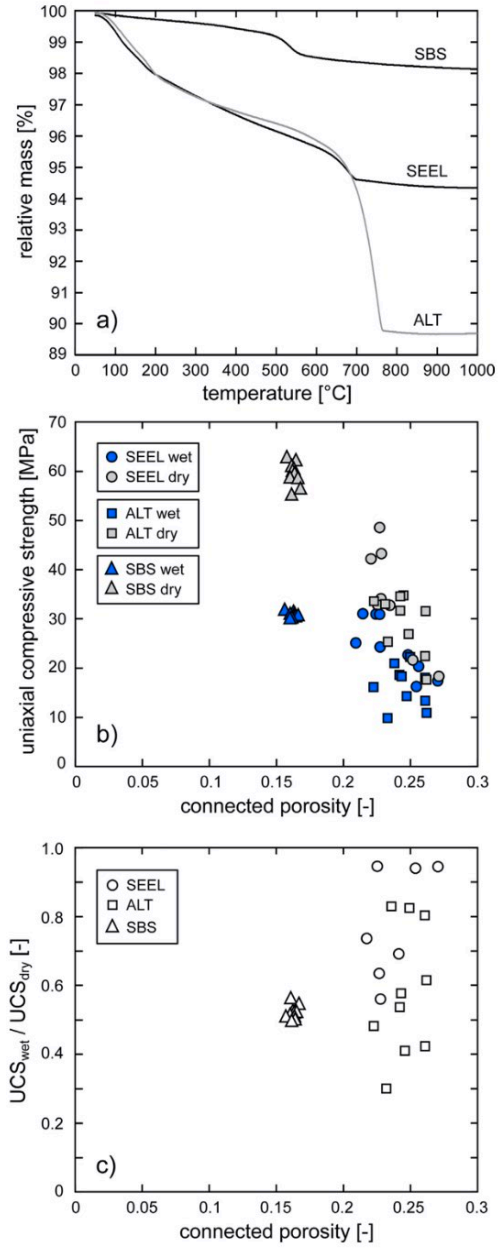

492

493 **Fig. 4**. (a) Relative mass as a function of temperature, measured using a Netzsch STA
494 449 C thermobalance apparatus. (b) Uniaxial compressive strength as a function of
495 connected porosity for the three rocks tested in this study. (c) The ratio of wet to dry
496 strength as a function of connected porosity for the three rocks tested in this study.
497 SBS—Schönbrunn sandstone. ALT—Altenbürg suevite. SEEL—Seelbronn suevite.
498 Wet—vacuum-saturated in deionised water (see text for details). Dry—dried in a
499 vacuum oven at 40 °C for at least 48 h. UCS_{wet}—wet uniaxial compressive strength.
500 UCS_{dry}—dry uniaxial compressive strength.